Molecular Biology Reports (2025) 52:413
https://doi.org/10.1007/s11033-025-10486-3

ORIGINAL ARTICLE

Chronic changes developing in the hydronephrotic and contralateral kidneys during unilateral ureteral obstruction in rats

Tuncer Kutlu[1] · Ufuk Kaya[2] · Ziya Yurtal[3] · Mehmet Güvenç[4] · Hüseyin Özkan[5] · Muhammed Etyemez[6] · İbrahim Alakuş[3] · Hasan Hüseyin Keçeli[5]

Received: 3 March 2025 / Accepted: 31 March 2025 / Published online: 22 April 2025

Abstract

Background Animal models of chronic kidney disease are important experimental tools used to validate new mechanisms and potential innovations, as well as to investigate therapeutic interventions before clinical trials in humans. This study aimed to determine the chronic changes occurring in the obstructed kidneys (OK) and the contralateral (CL) kidneys in unilateral ureteral obstruction (UUO) in rats.

Methods and results In the study, three groups (n:6) were formed. It was observed that dilated tubules decreased at 28 days compared to 14 days, while mononuclear cell infiltration and fibrosis increased. In the CL kidneys, glutathione (GSH) was lower compared to the control group (CG) at 14 days; at 28 days, malondialdehyde (MDA) was elevated, and GSH and catalase (CAT) levels were reduced. Nuclear factor erythroid 2–related factor 2 (NRF-2) protein expression was lower in the OK compared to the CL kidneys at both 14 and 28 days. NRF-2 gene expression was lower in the OK only at 28 days compared to the CG. However, in the CL kidneys, NRF-2 gene expression was higher at both 14 and 28 days compared to the CG. Cyclooxygenase-2 (COX-2) protein levels showed a significant increase in both the OK and CL kidneys at 14 days. COX-2 gene expression increased in the OK at 14 days compared to the CG. BAX protein levels were lower in the OK at 28 days compared to both the CG and CL kidneys. BCL-2 protein levels were lower in the OK compared to the CL kidneys at both 14 and 28 days.

Conclusion This study has identified changes in both the OK and CL kidneys, providing significant data for potential therapeutic, supportive, or protective research aimed at treating these kidneys.

Keywords BAX · BCL-2 · COX-2 · NRF-2 · Oxidative stress · UUO

Introduction

Chronic kidney disease is one of the fastest-growing causes of death, characterized by increased oxidative stress and chronic inflammation [1, 2]. The high prevalence of chronic kidney disease is due to the insufficiency of effective treatments for halting, preventing, and reversing renal fibrosis [1]. Animal models of chronic kidney disease are important experimental tools used to validate new mechanisms and potential innovations, as well as to investigate therapeutic interventions before clinical trials in humans [1, 3, 4].

The unilateral ureteral obstruction (UUO) model is a widely used method for elucidating the mechanisms of progressive kidney fibrosis [5–7]. Intensive research on the molecular mechanisms of UUO-induced renal fibrosis, inflammatory response, and oxidative stress continues and remains highly relevant [4]. Prolonged ureteral obstruction

✉ Tuncer Kutlu
tuncerkutlu83@gmail.com

1 Faculty of Veterinary Medicine, Department of Pathology, Hatay Mustafa Kemal University, Hatay 31300, Turkey

2 Faculty of Veterinary Medicine, Department of Biostatistics, Hatay Mustafa Kemal University, Hatay 31300, Turkey

3 Faculty of Veterinary Medicine, Department of Surgery, Hatay Mustafa Kemal University, Hatay 31300, Turkey

4 Faculty of Veterinary Medicine, Department of Physiology, Hatay Mustafa Kemal University, Hatay 31300, Turkey

5 Faculty of Veterinary Medicine, Department of Genetics, Hatay Mustafa Kemal University, Hatay 31300, Turkey

6 Faculty of Veterinary Medicine, Department of Physiology, Kastamonu University, Kastamonu 37150, Turkey

leads to a series of pathophysiological changes in the kidney, including fibroblast proliferation and activation, inflammation, oxidative stress, cytokine release, epithelial-mesenchymal transition, and extracellular matrix accumulation [4, 8].

Renal fibrosis frequently occurs not only in the obstructed kidneys (OK) but also in the contralateral (CL) kidneys in obstructive kidney disease, leading to renal dysfunction. The mechanisms of damage in the OK have been studied for years, and although its mechanisms are well understood, the pathogenesis of fibrosis in the CL kidney remains largely unknown [9]. Compensatory hypertrophy, similar to that seen in patients undergoing nephrectomy, occurs in the contralateral kidneys concurrent with the obstruction induced by experimental UUO [10]. The severity and duration of the obstruction induced by UUO determine the compensatory changes in the CL kidney [11].

Understanding the molecular mechanisms underlying obstruction-induced renal fibrosis and identifying novel therapeutic strategies is crucial; however, further studies are needed to prevent, slow, and treat the progression of kidney fibrosis [2, 4]. This study aimed to identify the changes occurring in both the OK and CL kidneys during the chronic phase using histopathological, biochemical, and molecular methods. Unlike many studies that focus only on early (7 days) or intermediate (14 days) changes, this study extends the timeline to 28 days, providing insights into progressive kidney damage [1, 3, 11].

Materials and methods

Animals and experimental protocol

In the study, 18 male Wistar Albino rats, aged 3 months and weighing 300–350 g, were used. This study was conducted with the approval of the Animal Experiments Local Ethics Committee of Hatay Mustafa Kemal University, under permission number 2022/06-14. Experimental procedures were conducted in accordance with the conditions for the care and use of laboratory animals (12 h light: 12 h dark and 24 ± 3 °C). During the experimental procedures, the rats were provided with standard commercial rat chow (pellet feed) and tap water ad libitum.

Three groups were formed, each consisting of six rats. The first group served as the control group (CG) and was euthanized on day 29 without any intervention. UUO surgery was performed on the other two groups to induce hydronephrosis, with the second group euthanized on day 15 and the third group on day 29.

In the UUO surgery performed to induce hydronephrosis, all rats were anesthetized with xylazine HCl (10 mg/kg, intraperitoneally [IP]) and ketamine HCl (50 mg/kg, IP). The abdominal areas of the anesthetized rats were shaved. The incision areas of the rats, positioned on their backs on the table, were aseptically prepared. After the midline incision, the abdominal cavity was accessed. After exposing the left kidney, the left ureter was identified. Two ligatures were placed on the midpoint of the left ureter using 5/0 non-absorbable sutures, and the ureter was transected between the ligatures. Subsequently, the peritoneum, muscles, and skin were routinely closed using 3/0 absorbable sutures [6, 12, 13].

Finally, the rats were euthanized under anesthesia by using xylazine HCl (10 mg/kg, IP) and ketamine HCl (50 mg/kg, IP). Following necropsy, the kidneys were excised, and the changes occurring in both the left kidneys and the compensatory right kidneys were investigated using pathological, molecular, and biochemical methods. The kidney of the ligated ureter is termed the Obstructed Kidney (OK) and the contralateral second kidney is termed contralateral (CL) kidney [6].

Histopathologic examination

At the end of the experiment, the kidneys were excised and placed in 10% buffered formalin for pathological examination. For histopathological examinations, the tissues were processed through alcohol and xylene series using routine methods, embedded in paraffin, and sectioned at 4 µm thickness. The sections were then deparaffinized in xylene, passed through 100, 96, 80, and 70% alcohol series, and stained with Hematoxylin and Eosin (H&E). Additionally, Masson's trichrome staining was performed for connective tissue, and Sirius red staining was applied for collagen. All microscopic findings were examined under a light microscope, and microphotographs were taken. Histopathological alterations in the kidneys, were assessed in five randomly selected areas (at 100× magnification), adhering to the criteria described by Otunctemur et al. [14], Hassan et al. [15] and Kutlu et al. [13]: 0 denoting no change, 1 indicating changes affecting < 25% of the area, 2 signifying changes affecting 25–50% of the area, and 3 representing changes affecting > 50% of the area.

Biochemical examination

To determine oxidative damage and antioxidant activity in kidney tissue, levels of malondialdehyde (MDA) and glutathione (GSH), as well as the activities of glutathione peroxidase (GSH-Px) and catalase (CAT), were evaluated spectrophotometrically.

For oxidative stress and antioxidant activity analyses, tissue samples were diluted at a ratio of 1/10 with Tris buffer (pH 7.4) and homogenized in a homogenizer. Total protein determination in the tissue was performed using the Lowry method [16].

The amount of MDA produced in the tissue was used as an indicator of lipid peroxidation levels. The MDA level was determined using the spectrophotometric method described by Placer et al. [17]. The pink-colored complex formed by MDA with thiobarbituric acid was measured spectrophotometrically at 532 nm, and the MDA level was expressed as nmol/g protein.

Tissue GSH levels were determined using the method described by Sedlak and Lindsay [18]. The color intensity of the yellow complex formed by the reaction of 5,5′-dithiobis (2-nitrobenzoic acid) with sulfhydryl groups was directly proportional to the GSH concentration in the sample. Therefore, the samples were measured spectrophotometrically at 412 nm, and the GSH level was expressed as nmol/g.

CAT activity in the tissue was determined using the method described by Goth [19]. When the tissue was incubated with a hydrogen peroxide (H_2O_2) containing substrate, H_2O_2 is broken down into H_2O and O_2 by catalase activity. Ammonium molybdate added to the medium reacts with H_2O to terminate the reaction. The color change occurring during this period was measured spectrophotometrically at 405 nm against a blank, and catalase enzyme activity was expressed as kU/g protein.

The activity of GSH-Px in the tissue was determined using the method described by Lawrence and Burk [20]. The yellow-colored complex formed by the samples with DTNB solution was read spectrophotometrically at 412 nm, and the GSH-Px enzyme activity level was expressed as IU/g protein.

Molecular examination

The tissues quickly frozen with liquid nitrogen were brought to the laboratory in liquid nitrogen and stored at − 80 °C until the analyses were performed. Total RNA isolation from kidney tissues was performed using a modified Trizol method with a commercial kit [21]. For this purpose, tissue samples stored at − 80 °C were exposed to 1 mL of TRIzol Reagent (Thermo Fisher, USA) and homogenized. After homogenization, the samples were left at room temperature for 10 min, and then 250 µl of chloroform was added followed by centrifugation. Then, the samples were sequentially treated with isopropyl alcohol and ethanol, and the RNA pellets were left to air-dry at room temperature for 10 min [22]. After drying, the RNA pellets of samples were diluted with 20 µl of nuclease-free water, and their purity and concentration values were determined using a nucleic acid spectrophotometer (Merinton SMA-1000, China). RNA quality of the samples were also checked by 1% agarose gel electrophoresis.

Following RNA isolation, a DNA digestion protocol (EN0521, DNase I, RNase free, Thermo Fischer Scientific, USA) was applied to eliminate potential genomic DNA before cDNA synthesis. Subsequently, cDNA synthesis was performed using the Onescript Plus cDNA synthesis kit (G236, ABM, USA) at 50 °C for 15 min, followed by 5 min at 85 °C through thermal cycler (T100, Biorad, USA). After cDNA synthesis, the samples were completed to 100 µl with nuclease-free water and stored at − 20 °C until further analysis.

Amplifications of target genes tumor necrosis factor-alpha (*TNFα)*, *COX-2*, *NRF2*, *BAX*, and *BCL-2*, as well as the *ACTB* housekeeping gene, were determined by Real-Time PCR (Rotorgene Q MDx 5plex, Qiagen, USA) in the samples. For this purpose, a commercial kit (EnTurbo™ SYBR Green PCR SuperMix, EQ014, ELK Biotechnology, China) containing SYBR Green dye was used. The qPCR reaction was set up with an initial denaturation at 95 °C for 10 min, followed by 40 cycles of 15 s at 95 °C, 60 s at 60 °C, and 30 s at 72 °C. In the study, the samples were loaded in duplicates. The primer sequences used for amplification of target genes were checked through Primer BLAST (NCBI) (Table 1).

In the study, the amounts of proteins encoded by target genes in the kidneys were determined using the ELISA method. For this purpose, the levels of the targeted proteins were determined using rat-specific TNFα (E-EL-R2856_ELABSCIENCE, USA) COX-2 (E-EL-R0792-ELABSCIENCE, USA), NRF2 (E-EL-R1052-ELABSCIENCE, USA), BAX (ER0512-FineTEST, China), and BCL-2 (ER762-FineTEST, China) ELISA kits. The total protein levels in the samples were measured using the BCA Assay Kit (23227, Thermo Fisher, USA). The protein levels in the target tissue were determined by normalizing to the total protein levels.

Statistical analysis

Before proceeding to significance tests, the variables were examined for normality using the Shapiro–Wilk test and for

Table 1 Forward and reverse sequences of studied genes

Gene	Forward and reverse sequences	References
ACTB	F:5′-GCAGGAGTACGATGAGTCCG-3′ R:5′-ACGCAGCTCAGTAACAGTCC-3′	[22]
TNF-α	F:5′-GGCATGGATCTCAAAGACAACC-3′ R:5′-CAAATCGGCTGACGGTGTG-3′	[23]
COX-2	F:5′-TGTATGCTACCATCTGGCTTCGG-3′ R:5′-GTTTGGAACAGTCGCTCGTCATC-3′	[23]
NRF-2	F:5′-TTGTAGATGACCATGAGTCGC-3′ R:5′-TGTCCTGCTGTATGCTGCTT-3′	[23]
BAX	F:5′-TGGCGATGAACTGGACAACAA-3′ R:5′-GGGAGTCTGTATCCACATCAGCA-3′	[24]
BCL-2	F:5′-TGGCCTTCTTTGAGTTCGGT-3′ R:5′-GATGCCGGTTCAGGTACTCA-3′	[25]

homogeneity of variances using the Levene test. In the study, the differences in histopathological findings between the groups were evaluated using the Kruskal–Wallis test with multiple Dunn test. The differences in oxidative damage and antioxidant activity variables and protein levels determined by the ELISA among the groups were determined using one-way ANOVA. For these parameters with statistically significant, Duncan's test was used as a post-hoc test. Gene expression analyses were calculated using the $2^{-\Delta\Delta Ct}$ method reported by Livak and Schmittgen [26] and presented as fold change. All statistical analyses were performed using the IBM SPSS 23.0 statistical software, and results was evaluated based on the criterion of $p < 0.05$.

Results

Macroscopically, the kidneys in the CG and the CL kidneys in the other groups had a normal structure. However, in the groups with UUO, it was observed that the volume of the obstructed kidneys had increased and they appeared pale in color. In these kidneys, it was observed that the renal pelvis had significantly dilated and hydronephrosis had developed.

Microscopically, the histopathological findings and their scores observed in the groups are presented in Table 2. In the CG, the kidneys exhibited a normal histological structure (Fig. 1a). In the UUO-induced OK, moderate cystic dilated tubules, mononuclear cell infiltration, and mild fibrosis with collagen accumulation were observed at 14 days, with statistically significant result (Fig. 1b–d). Cystic dilated tubules significantly decreased at 28 days compared to day 14, while mononuclear cell infiltration and fibrosis significantly increased (Fig. 1e–g). However, although the collagen amount increased, the increase was not significant (Fig. 1h). No lesions were observed in the contralateral kidneys, except for mild hyperemia, at both 14 and 28 days.

The levels of oxidative stress and antioxidant activity markers obtained at the end of the study are presented in Fig. 2. The MDA level in the OK showed an increase compared to the CGat both 14 and 28 days, although the increase was not statistically significant. In the CL kidneys, the MDA level showed a significant increase at 28 days compared to both the CG and OK. The GSH level, compared to the CG, showed a non-significant decrease in the OK at both 14 and 28 days, while a significant decrease was observed in the CL kidneys. No significant change was observed in the GSH-Px level. No significant decrease was observed in the CAT levels in the OK at both 14 and 28 days. In the CL kidneys, a non-significant decrease was observed at 14 days. At 28 days, a significant decrease was observed in the CL kidney.

A_{260}/A_{280} ratio (> 1.80) and concentration (> 500 ng/µL) of the isolated samples were suitable for cDNA synthesis and qPCR applications. Significant changes in the expression levels of target genes were detected at both 14 and 28 days compared to the CG. In the OK, the *COX-2* was approximately twofold upregulated at 14 days compared to theCG. Moreover, *NRF-2* was found to be down-regulated by an average of twofold at 28 days compared to the CG, while the expression levels of *TNF-α*, *BAX*, and *BCL-2* at 28 days were observed to be similar to those of the CG (Fig. 3).

In the CL kidneys, the *TNF-α* gene expression level at 14 days was found to be significantly downregulated compared to the CG ($P < 0.05$). On the other hand, *NRF-2* gene expression levels were found to be up-regulated more than twofold at both 14 and 28 days compared to the CG. Moreover, the *BCL-2* gene expression levels were

Table 2 Histopathologic findings and scoring were observed in the groups OK

Parameters	Group	Mean	Standard error of mean	Median	Minimum	Maximum	p
Mononuclear cell infiltration	Control	0.17 ^{C}	0.17	0.00	0.00	1.00	0.001
	14 Days	2.33 ^{B}	0.21	2.00	2.00	3.00	
	28 Days	3.00 ^{A}	0.00	3.00	3.00	3.00	
Cystic dilated tubules	Control	0.00 ^{C}	0.00	0.00	0.00	0.00	0.001
	14 Days	2.17 ^{A}	0.17	2.00	2.00	3.00	
	28 Days	1.33 ^{B}	0.21	1.00	1.00	2.00	
Fibrosis	Control	0.00 ^{C}	0.00	0.00	0.00	0.00	0.001
	14 Days	1.17 ^{B}	0.17	1.00	1.00	2.00	
	28 Days	2.17 ^{A}	0.31	2.00	1.00	3.00	
Collagen	Control	0.00 ^{B}	0.00	0.00	0.00	0.00	0.003
	14 Days	0.67 ^{A}	0.21	1.00	0.00	1.00	
	28 Days	1.17 ^{A}	0.17	1.00	1.00	2.00	

^{A,B,C}Different capital letters in rows indicate statistical significance between groups ($P<0.05$)

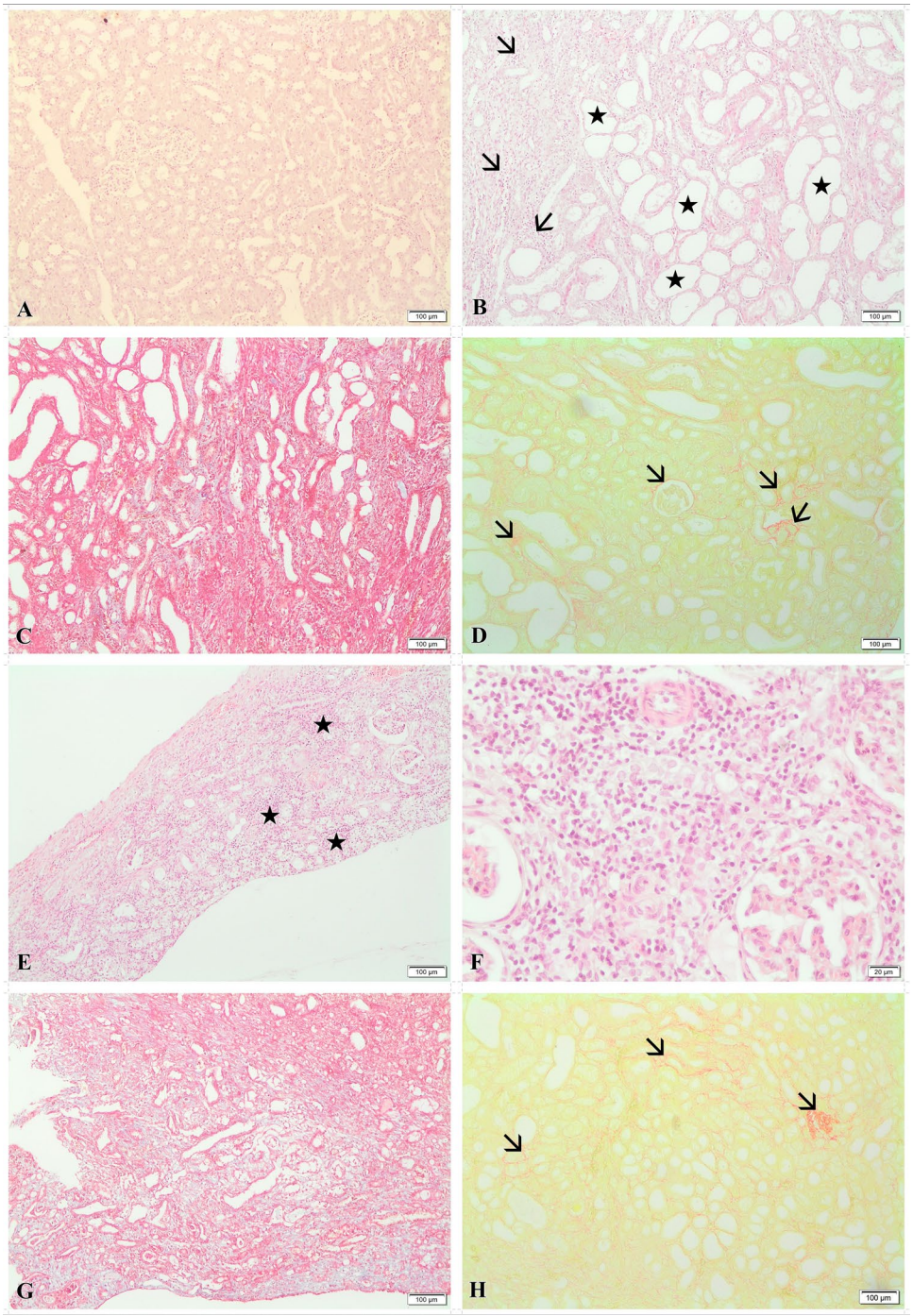

Fig. 1 Histopathological changes in the in the groups, **a** CG; normal kidney tissue. H&E. **b** 14 Days OK; moderate cystic dilated tubules (stars) and mononuclear cell infiltration (arrows), H&E. **c** 14 Days OK; mild fibrosis, Masson's trichrome. **d** 14 Days OK; mild collagen accumulation (arrows), Sirius red. **e** 28 Days OK; Severe mononuclear cell infiltration (stars). H&E. **f** 28 Days OK; Severe mononuclear cell infiltration. H&E. **g** 28 Days OK; moderate fibrosis, Masson's trichrome. **h** 28 Days OK; mild collagen accumulation (arrows), Sirius red

found to be significantly upregulated compared to the CG ($P < 0.05$) (Fig. 4).

The protein expression levels detected in the groups are presented in Fig. 5. In our study, NRF-2 protein expression was significantly lower in the OK of the same groups compared to the CL kidneys at both 14 and 28 days. The protein expression level of TNF-α in the OK showed a significant decrease compared to the CG and CL kidneys at both 14 and 28 days, while no significant change was observed in the CL kidneys.

The COX-2 protein level showed a significant increase in both the OK and CL kidneys at 14 days. However, at 28 days, values close to those of the CG were observed. The BAX protein level was lower in the OK at 28 days

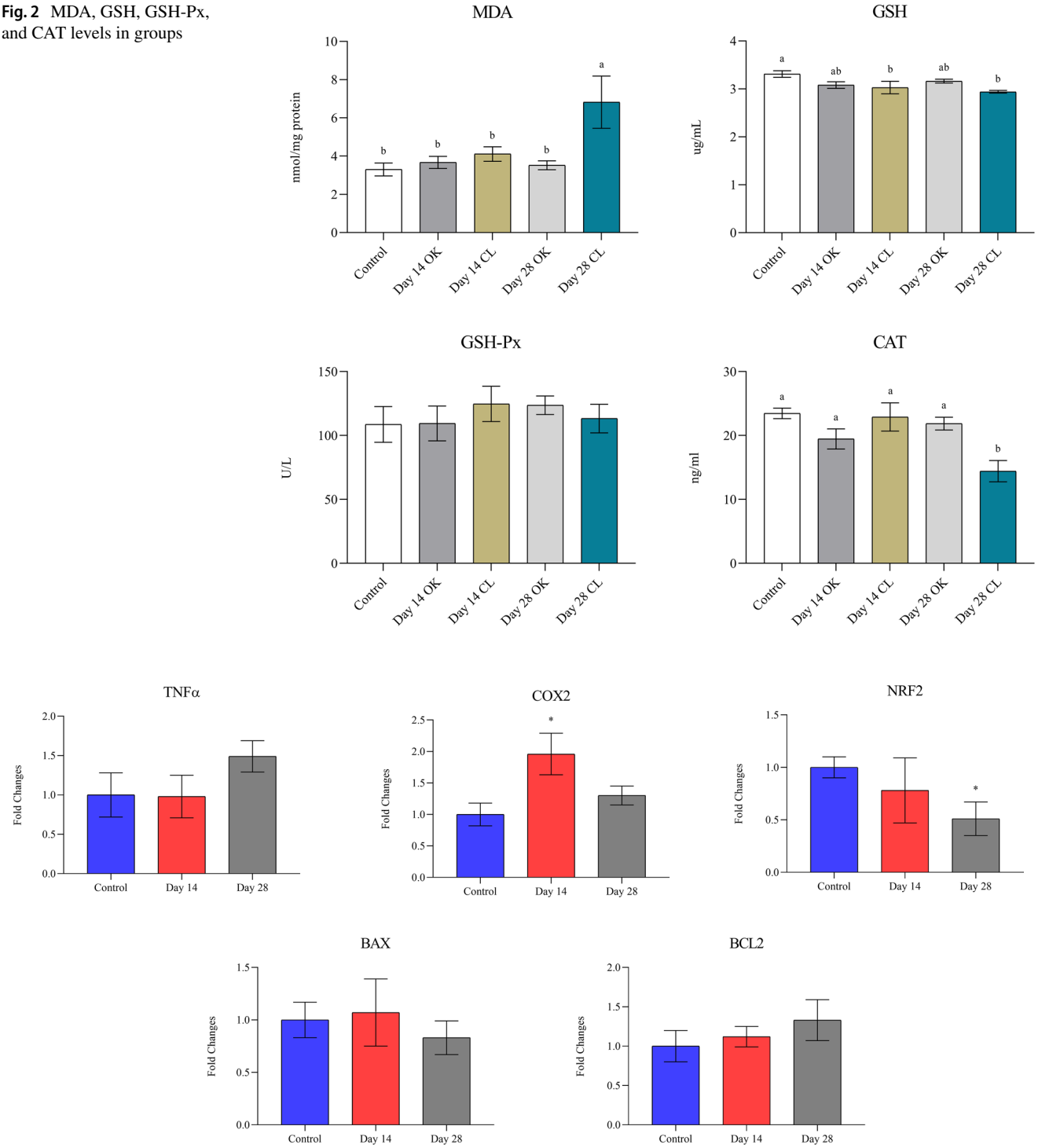

Fig. 2 MDA, GSH, GSH-Px, and CAT levels in groups

Fig. 3 Expressions of target genes in OK tissue

compared to both the CG and CL kidneys. The BCL-2 protein level was lower in the OK at both 14 and 28 days compared to the CL kidneys.

Discussion

UUO model studies are conducted for chronic kidney diseases, typically in the early phase at around 7 days or in

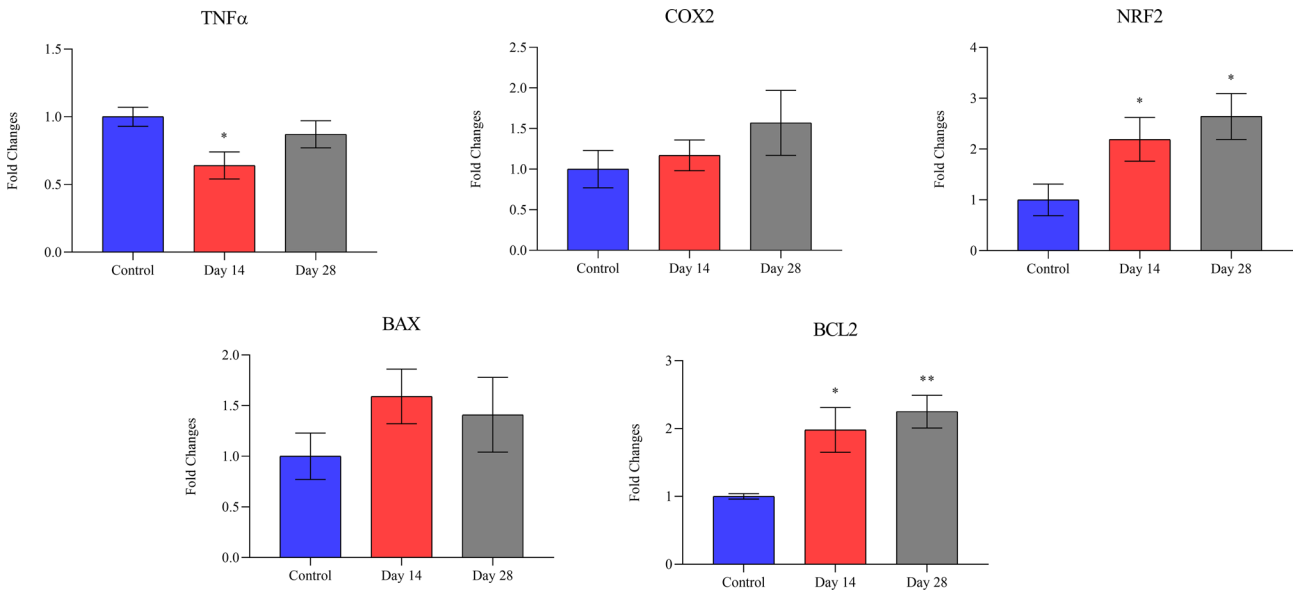

Fig. 4 Expressions of target genes in CL kidneys tissue

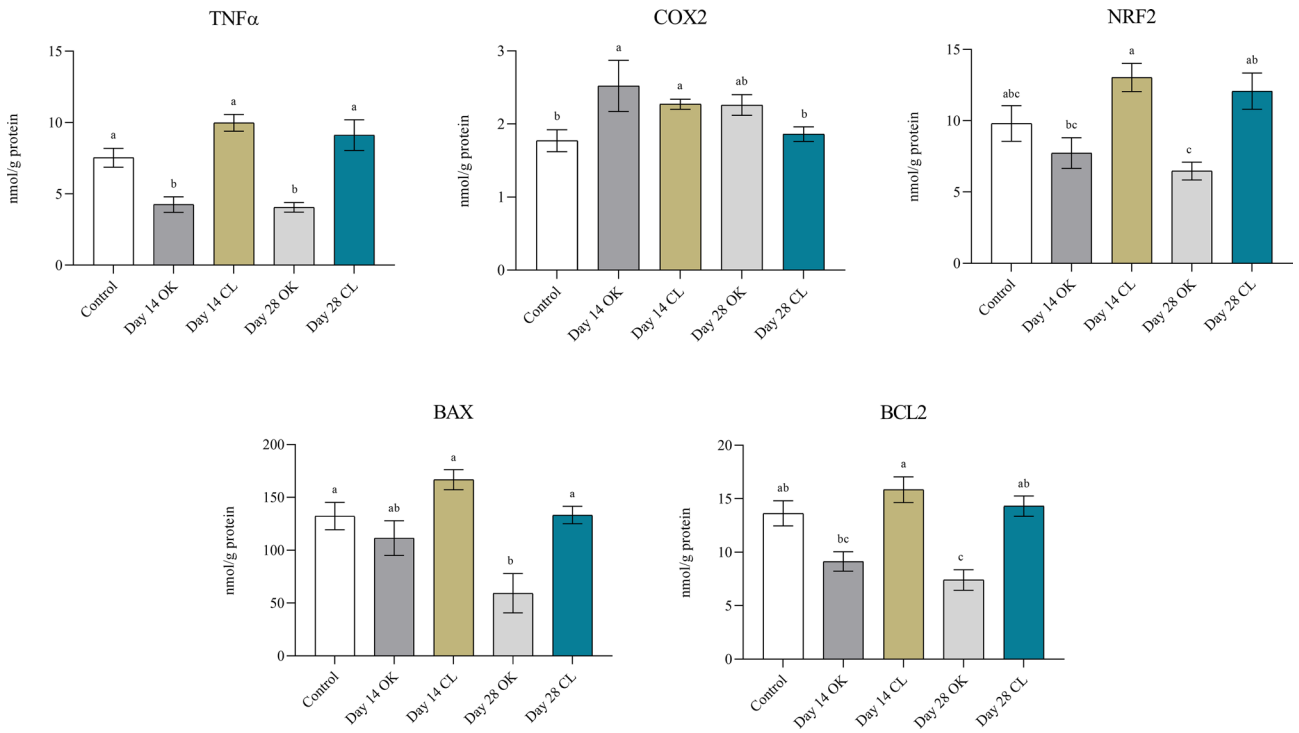

Fig. 5 The protein levels of, TNF-α, COX-2, NRF2, BAX and BCL2

later phases at 14 days or longer [1, 3, 11, 27]. In this study we investigated both the OK and CL kidneys, providing a holistic view of the impact of UUO including oxidative stress markers and gene expression alterations up to 28 days.

In UUO, a progressive increase in interstitial inflammatory cell infiltration occurs from 12 h to 14 days post-obstruction. This inflammation plays a significant role in the repair of obstruction-induced kidney injury and in the process of fibrosis [4, 7, 27]. Sulistiyowati et al.

[27] reported that by day 14, atrophic tubules and extensive interstitial areas filled with inflammatory cells and connective tissue cells were observed. In our study, an increase in mononuclear cell infiltration and fibrosis was observed at 14 days compared to the CG. Additionally, it was noted that this increase continued at 28 days compared to 14 days. Guo et al. [28] also stated that interstitial fibrosis emerges between 5 and 12 days and peaks at 19 days. In our study, it was also observed that the cystic dilated tubules present at 14 days decreased by 28 days. It was concluded that this condition resulted from the atrophy of tubules due to increased inflammatory cell infiltration and connective tissue cells.

In the UUO model, oxidative stress contributes to the progression of kidney damage from the early stages, and MDA levels, a marker of lipid peroxidation, increase following UUO [6, 15]. In this study, MDA levels increased in the OK kidneys, but the increase was not statistically significant. A significant increase in MDA levels was observed in the CL kidneys at 28 days.

It has been determined that UUO reduces renal antioxidant enzyme activation; in OK, antioxidants such as CAT and GSH, which protect against ROS-induced damage, were found to be lower compared to CL kidneys [15, 29]. Martínez-Klimova et al. [6] reported that in UUO, the antioxidant enzymatic system decreased and CAT levels declined by 14 days. However, in our study, it was observed that CAT levels in the OK remained similar to the CG at 14–28 days, while a significant decrease was noted only in the CL kidneys at 28 days. It was also observed that there was no change in GSH levels in the OK, but a significant decrease occurred in the CL kidneys compared to the CG. Based on these findings, it was concluded that oxidative stress occurs more significantly in the CL kidneys compared to the OK in such conditions. Additionally, it was concluded that the increase in MDA levels and the decrease in CAT and GSH levels in the CL kidneys were due to adaptation and compensation mechanisms.

NRF-2 is a transcription factor that plays a key role in protection against oxidative stress and the regulation of inflammatory responses. Preclinical and clinical studies have shown that strategies targeting NRF-2 activation prevent the progression of chronic kidney disease and protect against acute kidney injury [2]. In the UUO model, RAS activation and increased Nuclear Factor κB (NF-κB) can downregulate NRF2 expression in rat kidneys [30]. RAS activation is likely the inducer of increased ROS production by Nox and the suppression of NRF-2 [6, 31]. In our study, NRF-2 protein expression in OK was significantly lower compared to CL kidneys in the same groups at both 14 and 28 days. In terms of NRF-2 gene expression, it was lower in OK compared to the CGonly at 28 days. However, in CL kidneys, NRF-2 gene expression was significantly higher compared to the CG at both 14 and 28 days. It was concluded that this also contributed to the adaptation process in CL kidneys.

Renal TNF-α levels increase in the early phase of UUO [29]. Prud'homme et al. [32] determined that plasma levels of TNF-α significantly increased in the UUO model, reaching a maximum peak at 28 days. Additionally, increased macrophage infiltration and cytokine production, along with the upregulation of TNF-α, promote severe renal inflammation and fibrosis, indicating that inflammation plays a significant role in obstruction-induced kidney injury [7, 33]. Furthermore, RAS activation stimulates the production of factors such as TNF-α, which trigger leukocyte migration and the inflammatory process [6]. However, in our study, it was notable that TNF-α protein expression decreased in OK compared to both CG and CL kidneys at both 14 and 28 days. In terms of gene expression, a significant decrease was observed in CL kidneys only at 14 days.

UUO in rodents is a widely used experimental model of renal fibrosis. In obstructed kidneys, increased production of prostaglandin E2 (PGE2) has been reported [6, 34]. Increased PGE2 synthesis is associated with elevated COX-2 expression in the UUO model [35]. In vitro evidence shows that COX-2 expression in renal medullary interstitial cells increases in response to pressure, dependent on endogenous reactive oxygen species (ROS) production [36]. It is stated that COX-2 plays a protective role against tubulointerstitial fibrosis during UUO [34]. In our study, COX-2 protein levels showed a significant increase in both OK and CL kidneys at 14 days. In OK, COX-2 gene expression also showed an approximately twofold upregulation compared to the CG at 14 days. Other studies have also shown that ureteral obstruction significantly increases COX-2 expression [34, 37, 38].

UUO results in widespread tubular apoptosis in obstructed kidneys of both adults and neonates. The oncoprotein BCL-2 inhibits several forms of apoptosis, while the related protein Bax promotes apoptosis. It has been stated that chronic UUO inhibits BCL-2 expression in selected tubules of the obstructed kidney, which contributes to the activation of apoptosis and progressive kidney damage in both neonatal and adult kidneys. The activation of apoptosis is dependent on the relative balance between BCL-2 and BAX [39, 40].

In our study, BCL-2 protein levels were lower in OK compared to CL kidneys at both 14 and 28 days. In CL kidneys, BCL-2 gene expression levels were significantly upregulated compared to the CG. BAX protein levels were lower in OK compared to both CG and CL kidneys only at 28 days.

In our study effectively examinated both OK and CL kidneys, providing a holistic view of the impact of UUO. Although molecular and histopathological markers were studied, functional assessments (e.g. renal function tests, blood urea nitrogen, creatinine) were not included, which is a missing detail of this study.

Conclusion

The high prevalence of chronic kidney disease is due to the insufficient availability of effective treatments for halting, preventing, and reversing renal fibrosis [1]. This research will provide insights into the pathophysiology of fibrosis in OK and contribute to investigations aimed at protection and treatment in OK. Additionally, changes occurring in the compensation of CL kidneys have been identified, providing valuable data for research aimed at supporting or protecting these kidneys. Finally, this study adds some uniqueness by evaluating histopathological, biochemical and molecular markers together in a chronic setting.

Acknowledgements This study was presented as an oral presentation at the 9th International Congress on Veterinary and Animal Sciences and its abstract was printed in the congress booklet.

Author contribution T.K.: Project administration; conceptualization; funding acquisition; data curation; investigation; methodology; visualization; writing—original draft. U.K.: Formal analysis; methodology; investigation; validation. Z.Y. and İ.A.: Investigation; methodology; writing—review and editing. M.G. and M.E.: Formal analysis; funding acquisition; funding acquisition; funding acquisition; software; writing—review and editing. H.Ö. and H.H.K.: Conceptualization; funding acquisition; methodology; resources; supervision; writing—review and editing. All authors reviewed and approved the manuscript.

Funding This research received no specific grant from any funding agency in the public, commercial, or not-for-profit sectors.

Data availability No datasets were generated or analysed during the current study.

Declarations

Conflict of Interest The authors declared that they have no competing interests.

Ethical approval This study was done with Hatay Mustafa Kemal University Animal Experiments Local Ethics Committee's permission numbered 2022/06-014.

References

1. Eddy AA, López-Guisa JM, Okamura DM, Yamaguchi I (2012) Investigating mechanisms of chronic kidney disease in mouse models. Pediatr Nephrol 27:1233–1247. https://doi.org/10.1007/s00467-011-1938-2
2. Guerrero-Hue M, Rayego-Mateos S, Vázquez-Carballo C, Palomino-Antolín A, García-Caballero C, Opazo-Rios L, Moreno JA (2020) Protective role of Nrf2 in renal disease. Antioxidants 10(1):39. https://doi.org/10.3390/antiox10010039
3. Bianco M, Lopes JA, Beiral HJ, Filho JD, Frankenfeld SP, Fortunato RS, Takiya CM (2019) The contralateral kidney presents with impaired mitochondrial functions and disrupted redox homeostasis after 14 days of unilateral ureteral obstruction in mice. PLoS ONE 14(6):e0218986. https://doi.org/10.1371/journal.pone.0218986
4. Wang Y, Deng X, Yang Z, Wu H (2023) Global research trends in unilateral ureteral obstruction-induced renal fibrosis: a bibliometric and visualized study. Medicine 102(32):e34713. https://doi.org/10.1097/MD.0000000000034713
5. Chevalier RL, Forbes MS, Thornhill BA (2009) Ureteral obstruction as a model of renal interstitial fibrosis and obstructive nephropathy. Kidney Int 75(11):1145–1152. https://doi.org/10.1038/ki.2009.86
6. Martínez-Klimova E, Aparicio-Trejo OE, Tapia E, Pedraza-Chaverri J (2019) Unilateral ureteral obstruction as a model to investigate fibrosis-attenuating treatments. Biomolecules 9(4):141. https://doi.org/10.3390/biom9040141
7. Prieto-Carrasco R, Silva-Palacios A, Rojas-Morales P, Aparicio-Trejo OE, Medina-Reyes EI, Hernández-Cruz EY, Pedraza-Chaverri J (2021) Unilateral ureteral obstruction for 28 days in rats is not associated with changes in cardiac function or alterations in mitochondrial function. Biology 10(7):671. https://doi.org/10.3390/biology10070671
8. Lu M, Li H, Liu W (2021) Curcumin attenuates renal interstitial fibrosis by regulating autophagy and retaining mitochondrial function in unilateral ureteral obstruction rats. Basic Clin Pharmacol Toxicol 128:594–604. https://doi.org/10.1111/bcpt.13550
9. Xiong Y, Chang Y, Hao J, Zhang C, Yang F, Wang Z, Xu Q (2021) Eplerenone attenuates fibrosis in the contralateral kidney of UUO rats by preventing macrophage-to-myofibroblast transition. Front Pharmacol 12:620433. https://doi.org/10.3389/fphar.2021.620433
10. Dicker SE, Shirley DG (1972) Compensatory hypertrophy of the contralateral kidney after unilateral ureteral ligation. J Physiol 220(1):199–210. https://doi.org/10.1113/jphysiol.1972.sp009701
11. Kubik MJ, Wyczanska M, Gasparitsch M, Keller U, Weber S, Schaefer F, Lange-Sperandio B (2020) Renal developmental genes are differentially regulated after unilateral ureteral obstruction in neonatal and adult mice. Sci Rep 10(1):19302. https://doi.org/10.1038/s41598-020-76328-3
12. Zhao J, Wang L, Cao A, Jiang M, Chen X, Peng W (2015) Renal tubulointerstitial fibrosis: a review in animal models. J Integr Nephrol Androl 2(3):75–80. https://doi.org/10.4103/2225-1243.161428
13. Kutlu T, Ozkan H, Yurtal Z, Kaya U, Guvenc M (2025) Morphological and molecular changes in renal tissue following experimental unilateral ureteral obstruction in rat kidneys. Kafkas Univ Vet Fak Derg 31(1):39–47. https://doi.org/10.9775/kvfd.2024.32776
14. Otunctemur A, Ozbek E, Cakir SS, Dursun M, Cekmen M, Polat EC, Ozcan L, Somay A, Ozbay N (2015) Beneficial effects montelukast, cysteinyl-leukotriene receptor antagonist, on renal damage after unilateral ureteral obstruction in rats. Int Braz J Urol 41(2):279–287. https://doi.org/10.1590/S1677-5538.IBJU.2015.02.14
15. Hassan NM, Said E, Shehatou GS (2021) Nifuroxazide suppresses UUO-induced renal fibrosis in rats via inhibiting STAT-3/NF-κB signaling, oxidative stress and inflammation. Life Sci 272:119241. https://doi.org/10.1016/j.lfs.2021.119241
16. Lowry OH, Rosenbrough NJ, Farr AL (1951) Protein measurement with the folin phenol reagent. J Biol Chem 193:265–275
17. Placer ZA, Cushman LL, Johnson BC (1966) Estimation of product of lipid peroxidation (malonyldialdehyde) in biochemical systems. Anal Biochem 16:359–364
18. Sedlak J, Lindsay RH (1968) Estimation of total, protein-bound, and nonprotein sulfhydryl groups in tissue with Ellman's reagent. Anal Biochem 25:192–205
19. Goth LA (1991) Simple method for determination of serum catalase activity and revision of reference range. Clin Chim Acta 196:143–151. https://doi.org/10.1016/0009-8981(91)90067-M

20. Lawrence RA, Burk RF (1976) Glutathione peroxidase activity in selenium-deficient rat liver. Biochem Biophys Res Commun 71:952–958. https://doi.org/10.1016/0006-291X(76)90747-6
21. Rio DC, Ares M, Hannon GJ, Nilsen TW (2010) Purification of RNA using TRIzol (TRI reagent). Cold Spring Harbor Protocols 6:pdb-prot5439. https://doi.org/10.1101/pdb.prot5439
22. Ozkan H, Kerman E (2020) Comparative evaluation of RNAlater solution and snap Frozen methods for gene expression studies in different tissues. Rev Romana Med Lab 28(3):287–297. https://doi.org/10.2478/rrlm-2020-0024
23. Güvenç M, Cellat M, Özkan H, Tekeli İO, Uyar A, Gökçek İ, İşler CT, Yakan A (2019) Protective effects of tyrosol against DSS-induced ulcerative colitis in rats. Inflammation 42(5):1680–1691. https://doi.org/10.1007/s10753-019-01028-8
24. Xu Q, Li YC, Du C, Wang LN, Xiao YH (2021) Effects of apigenin on the expression of LOX-1, Bcl-2, and Bax in hyperlipidemia rats. Chem Biodivers 18(8):e2100049. https://doi.org/10.1002/cbdv.202100049
25. Yun S, He X, Zhang W, Chu D, Feng C (2020) Alleviation effect of grape seed proanthocyanidins on neuronal apoptosis in rats with iron overload. Biol Trace Elem Res 194(1):210–220. https://doi.org/10.1007/s12011-019-01766-8
26. Livak KJ, Schmittgen TD (2001) Analysis of relative gene expression data using real-time quantitative PCR and the $2^{-\Delta\Delta CT}$ method. Methods 25(4):402–408. https://doi.org/10.1006/meth.2001.1262
27. Sulistiyowati I, Yunus J, Sari DCR, Arfian N (2020) Upregulation of p16, Bax and Bcl-2 mRNA expression associated with epithelial apoptosis and myofibroblast proliferation in kidney fibrosis model in mice. Malays J Med Sci 27(2):37–44. https://doi.org/10.21315/mjms2020.27.2.4
28. Guo YC, Zhang M, Wang FX, Pei GC, Sun F, Zhang Y (2017) Macrophages regulate unilateral ureteral obstruction-induced renal lymphangiogenesis through C-C motif chemokine receptor 2–dependent phosphatidylinositol 3-kinase-AKT–mechanistic target of rapamycin signaling and hypoxia-inducible factor-1α/vascular endo. Am J Pathol 187(8):1736–1749. https://doi.org/10.1016/j.ajpath.2017.04.007
29. Grande MT, Pérez-Barriocanal F, López-Novoa JM (2010) Role of inflammation in tubulo-interstitial damage associated to obstructive nephropathy. J Inflamm 7(1):1–14. https://doi.org/10.1186/1476-9255-7-19
30. Bolati D, Shimizu H, Yisireyili M, Nishijima F, Niwa T (2013) Indoxyl sulfate, a uremic toxin, downregulates renal expression of Nrf2 through activation of NF-κB. BMC Nephrol 14(56):1–9. https://doi.org/10.1186/1471-2369-14-56
31. Sedeek M, Nasrallah R, Touyz RM, Hebert RL (2013) NADPH oxidases, reactive oxygen species, and the kidney: friend and foe. J Am Soc Nephrol 24:1512–1518. https://doi.org/10.1681/ASN.2012111112
32. Prud'homme M, Coutrot M, Michel T, Boutin L, Genest M, Poirier F, Launay JM, Kane B, Kinugasa S, Prakoura N, Vandermeersch S, Cohen-Solal A, Delcayre C, Samuel JL, Mehta R, Gayat E, Mebazaa A, Chadjichristos CE, Legrand M (2019) Acute kidney ınjury ınduces remote cardiac damage and dysfunction through the Galectin-3 pathway. JACC Basic Transl Sci 4:717–732. https://doi.org/10.1016/j.jacbts.2019.06.005
33. Wen Y, Lu X, Ren J, Privratsky JR, Yang B, Rudemiller NP, Zhang J, Griffiths R, Jain MK, Nedospasov SA, Liu BC, Crowley SD (2019) KLF4 in macrophages attenuates TNFα-mediated kidney ınjury and fibrosis. J Am Soc Nephrol 30:1925–1938. https://doi.org/10.1681/ASN.2019020111
34. Yang T, Li C (2016) Role of COX-2 in unilateral ureteral obstruction: what is new? Am J Physiol Renal Physiol 310(8):746–747. https://doi.org/10.1152/ajprenal.00498.2015
35. Kamata M, Hosono K, Fujita T, Kamata K, Majima M (2015) Role of cyclooxygenase-2 in the development of interstitial fibrosis in kidneys following unilateral ureteral obstruction in mice. Biomed Pharmacother 70:174–180. https://doi.org/10.1016/j.biopha.2015.01.010
36. Ostergaard M, Christensen M, Nilsson L, Carlsen I, Frokiaer J, Norregaard R (2014) ROS dependence of cyclooxygenase-2 induction in rats subjected to unilateral ureteral obstruction. Am J Physiol Renal Physiol 306:259–270. https://doi.org/10.1152/ajprenal.00352.2013
37. Jia Z, Wang N, Aoyagi T, Wang H, Liu H, Yang T (2011) Amelioration of cisplatin nephrotoxicity by genetic or pharmacologic blockade of prostaglandin synthesis. Kidney Int 79:77–88. https://doi.org/10.1038/ki.2010.331
38. Honma S, Takahashi N, Shinohara M, Nakamura K, Mitazaki S, Abe S, Yoshida M (2013) Amelioration of cisplatin-induced mouse renal lesions by a cyclooxygenase (COX)-2 selective inhibitor. Eur J Pharmacol 715:181–188. https://doi.org/10.1016/j.ejphar.2013.05.023
39. Chevalier RL, Smith CD, Wolstenholme J, Krajewski S, Reed JC (2000) Chronic ureteral obstruction in the rat suppresses renal tubular Bcl-2 and stimulates apoptosis. Exp Nephrol 8(2):115–122. https://doi.org/10.1159/000020657
40. Huang F, Huang S, Sun K, Chen Y, Xie G, Bao J, Fan Y (2025) Protective effect of compound K against podocyte injury in chronic kidney disease by maintaining mitochondrial homeostasis. Sci Rep 15(1):435. https://doi.org/10.1038/s41598-024-84704-6